

OPEN

Metabolomic Profiles of Bovine Mammary Epithelial Cells Stimulated by Lipopolysaccharide

Yixin Huang^{1,2,3,5}, Liuhong Shen^{1,2,5}, Jing Jiang^{1,2}, Qipin Xu^{1,2}, Zhengzhong Luo^{1,2}, Qiao Luo^{1,2}, Shumin Yu^{1,2}, Xueping Yao^{1,2}, Zhihua Ren^{1,2}, Yanchun Hu^{1,2}, Yongxin Yang⁴ & Suizhong Cao^{1,2*}

Bovine mammary epithelial cells (bMECs) are the main cells of the dairy cow mammary gland. In addition to their role in milk production, they are effector cells of mammary immunity. However, there is little information about changes in metabolites of bMECs when stimulated by lipopolysaccharide (LPS). This study describes a metabolomics analysis of the LPS-stimulated bMECs to provide a basis for the identification of potential diagnostic screening biomarkers and possible treatments for bovine mammary gland inflammation. In the present study, bMECs were challenged with 500 ng/mL LPS and samples were taken at 0 h, 12 h and 24 h post stimulation. Metabolic changes were investigated using high performance liquid chromatography-quadrupole time-of-flight mass spectrometry (HPLC-Q-TOF MS) with univariate and multivariate statistical analyses. Clustering and metabolic pathway changes were established by MetaboAnalyst. Sixty-three differential metabolites were identified, including glycerophosphocholine, glycerol-3-phosphate, L-carnitine, L-aspartate, glutathione, prostaglandin G₂, α -linolenic acid and linoleic acid. They were mainly involved in eight pathways, including D-glutamine and D-glutamic acid metabolism; linoleic acid metabolism; α -linolenic metabolism; and phospholipid metabolism. The results suggest that bMECs are able to regulate pro-inflammatory, anti-inflammatory, antioxidation and energy-producing related metabolites through lipid, antioxidation and energy metabolism in response to inflammatory stimuli.

Bovine mastitis is common and is economically one of the most important diseases that seriously affects the health and welfare of dairy cows. It is an inflammatory condition of the mammary gland, reducing milk quality and production, impairing fertility, causing mortality^{1,2}, and is a food-borne disease that increases human public health risks³.

Bovine mastitis is commonly caused by bacteria including *Staphylococcus aureus*, *Escherichia coli* and *Streptococcus*^{2,3}. LPS, the major component of the outer membrane of gram-negative bacteria, is a bacterial virulence factors that can induce strong immune responses in animals. In mammary gland, bMECs are important milk-producing cells and key regulators of immunity³⁻⁵. Research on bMECs is not only conducive to the understanding of growth and development of mammary gland and regulation of lactation, but also to a deeper understanding of mammary immunity. Thus LPS-stimulated bMECs have been widely used in studying bMECs immune response mechanisms or bovine mastitis.

Studies have shown that stimulation of bMECs with LPS can generate strong immune responses, upregulating the expression of pathogen-associated molecular patterns (PAMPs), activating nuclear factor- κ B (NF- κ B) signaling pathway, and increasing the secretion of inflammatory cytokines^{3,5}. In a study of bMECs⁴, the mRNA expression levels of Toll-like receptor 4 (*TLR4*) and *TLR2* were significantly increased by stimulation with 0.01 μ g/mL, 1 μ g/mL, 5 μ g/mL and 10 μ g/mL LPS for 24 h when compared to controls (without LPS). Significant upregulation of *TLR4* or *TLR2* mRNA expression was observed as early as 6 h ($p < 0.05$) or 24 h ($p < 0.01$) respectively

¹Department of Clinical Veterinary Medicine, College of Veterinary Medicine, Sichuan Agricultural University, Chengdu, 611130, China. ²Sichuan Provincial Key Laboratory of Animal Diseases and Human Health, Chengdu, 611130, China. ³Institute of Biodiversity Animal Health & Comparative Medicine, College of Medical, Veterinary & Life Sciences, University of Glasgow, Glasgow, G61 1QH, UK. ⁴Institute of Animal Science and Veterinary Medicine, Anhui Academy of Agricultural Sciences, Hefei, 230031, China. ⁵These authors contributed equally: Yixin Huang and Liuhong Shen. *email: suizhongcao@126.com

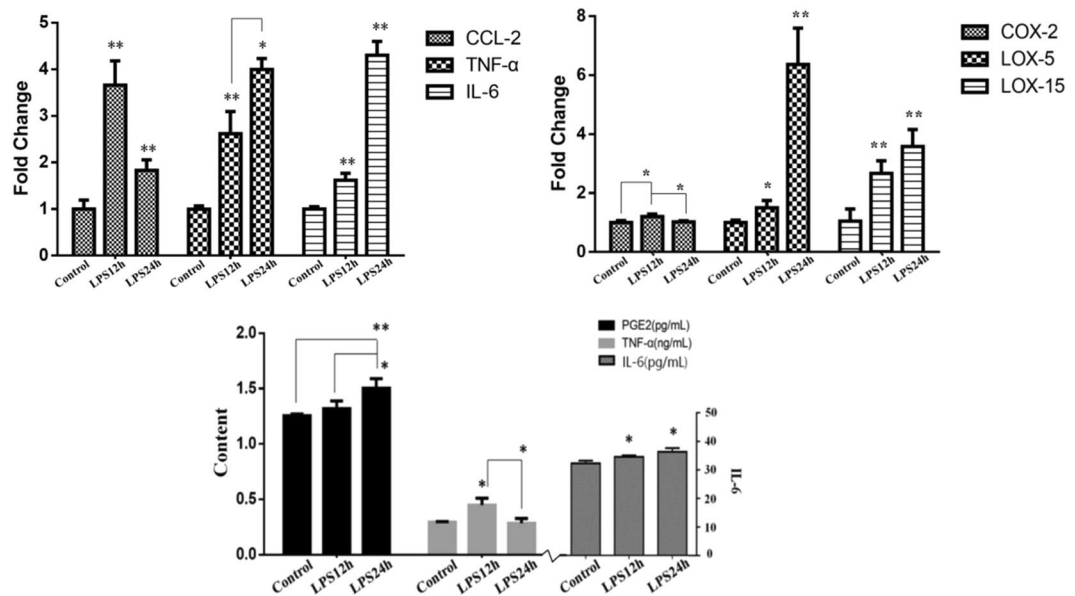


Figure 1. The mRNA (RT-qPCR) and protein (ELISA) expression of cytokines and enzymes. *Means $p < 0.05$, **means $p < 0.01$ ($n = 3$). It represents that the treatment group is compared with Control if there is no special indication.

after stimulation of $1 \mu\text{g/mL}$ LPS. Wu *et al.*⁵ found that after bMECs were stimulated with $10 \mu\text{g/mL}$ LPS for 12 h, the gene and protein expression levels of TLR4, NF- κ B p65 and NF- κ B p65 phosphorylation were significantly increased ($p < 0.05$). The mRNA expression of interleukin- 1β (*IL-1 β*), *IL-6*, tumor necrosis factor- α (*TNF- α*), inducible nitric oxide synthase (*iNOS*) and *NO* content increased significantly ($p < 0.05$) as well. After 10 ng/mL LPS stimulation for 24 h in bMECs¹, mRNA transcription of the enzymes responsible for arachidonic acid (AA) metabolism increased significantly, including prostaglandin (PG)-F synthase ($p < 0.001$), prostaglandin-endoperoxide synthase 2 and PGE synthase ($p < 0.01$). $\text{PGF}_{2\alpha}$ ($p < 0.01$), leukotriene - B_4 ($p < 0.05$) and LTC_4 ($p < 0.001$) secretion in bMECs were all increased. Differentially expressed proteins that were associated with inflammatory model of bMECs induced by LPS were screened by isobaric tag for relative and absolute quantification (iTRAQ), combined with 2-dimensional liquid chromatography- tandem mass spectrometry (2D-LC-MS/MS), indicating that LPS treatment could affect the synthesis of protein and fat in bMECs⁶. However, there is little information about changes in metabolite levels of bMECs when they are stimulated by LPS.

In this study, our aim was to identify potential biomarkers for the diagnosis and treatment of bovine mammary gland inflammation. Previous studies showed that pro-inflammatory cytokines usually promote inflammation quickly after the recognition of the pathogen, and then anti-inflammatory cytokines suppress and limit their activity³. The expression of mRNA and proteins of cytokines including *IL-6*, *TNF- α* , and enzymes including cyclooxygenase (COX) - 2, lipoxygenase (LOX) - 5 were measured in a pilot study, which suggested that 500 ng/mL of LPS and two time-points (12 h and 24 h after LPS stimulation) would be suitable for our study. We then used HPLC-Q-TOF MS technique, with the aim of identifying differentially produced metabolites and the relevant pathways of the inflammatory response in bMECs after LPS stimulation.

Results

The mRNA and protein expression of cytokines and enzymes. To determine the inflammatory conditions of bMECs, changes of several genes and proteins were investigated (Fig. 1). We found that the mRNA expression of chemokine (c-c motif) ligand (*CCL-2*), *IL-6* and *TNF- α* in LPS12h increased significantly ($p < 0.01$) compared to Control. When compared LPS24h with LPS12h, the mRNA expression of *IL-6* and *TNF- α* increased, while *CCL-2* decreased but it was still higher than that in Control ($p < 0.01$). In LPS12h, the mRNA expression of enzymes *COX-2*, *LOX-5* and *LOX-15* were up-regulated significantly when compared with Control. In LPS24h, the mRNA expression of *COX-2* decreased significantly when compared with LPS12h. The mRNA expression of *LOX-5* and *LOX-15* increased significantly ($p < 0.01$) when compared with Control. The results of protein expression showed that the secretion of *IL-6*, *TNF- α* and PGE2 increased in LPS12h compared to Control. When compared LPS24h with Control, the secretion of PGE2 and *IL-6* were up-regulated significantly. There was a significant drop of *TNF- α* in LPS24h compared to LPS12h. These results indicated that 500 ng/mL of LPS and two time-points (12 h and 24 h after LPS stimulation) were suitable for our study to establish an inflammatory model of bMECs.

Metabolic profiles. Representative HPLC-Q-TOF MS electrospray ionization (ESI) \pm chromatograms are shown in Supplementary Fig. S1. 3112 peaks and 4773 peaks were extracted in ESI- and ESI+, respectively. Figure 2 displays the similarities and differences among Control (green circles), LPS12h (blue circles) and LPS24h (red circles) in the score plots of PCA (principal component analysis). The quality control (QC) samples (yellow

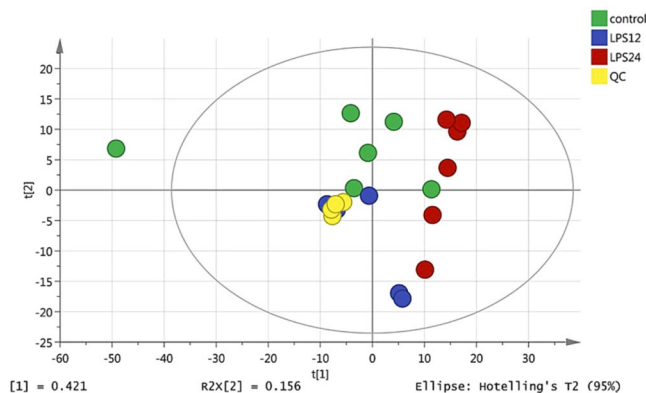


Figure 2. PCA score plots of three groups (with QC).

Groups	ESI+		ESI-	
	R2Y	Q2	R2Y	Q2
LPS12h-Control	1	0.883	0.999	0.826
LPS24h-Control	1	0.943	0.999	0.789
LPS24h-LPS12h	0.984	0.787	0.994	0.64

Table 1. Evaluation Parameters of OPLS-DA models. R2Y represents the rate of model interpretation, and Q2 represents the model predictive ability.

circles) were tightly clustered, indicating that the method used was robust, with high repeatability and stability. Supplementary Fig. S2 shows the results of partial least squares discriminant analysis (PLS-DA), in which the samples were aggregated within treatments, which were mostly distinct from each other. Table 1 and Fig. 3 are orthogonal partial least squares discriminant analysis (OPLS-DA) results, indicating that the model was stable and reliable, with good predictability.

Discovery and identification of the differential metabolites. According to the variable importance in projection (VIP) value obtained by OPLS-DA and the results of *t*-tests, metabolites that had both $VIP > 1$ and $p < 0.05$ were selected as significantly differential metabolites. A total of 63 metabolites at significantly different abundance according to treatment were identified, including 18 nucleotides and their derivatives, 22 lipids, 13 organic acids and their derivatives, and 10 other organic compounds. Among them, 10 same metabolites changed significantly both in LPS12h and LPS24h when compared to Control; 10 same metabolites were found to be different in Control vs LPS12h and LPS24h vs LPS12h; 8 were found to be different both in Control vs LPS24h and LPS12h vs LPS24h; 7 same metabolites differed in all three treatment groups (Fig. 4).

Hierarchical clustering of differential metabolites was performed by MetaboAnalyst 4.0 (Fig. 5). It showed that related metabolites and the treatment groups were clustered together. Some metabolites in bMECs in treatments LPS12h and LPS24h showed highly significant increases when compared with Control samples ($p < 0.01$), and were significantly up-regulated in LPS24h compared with LPS12h ($p < 0.05$). These included PC (18:1(9Z)/18:1(9Z)), sn-glycerol 3-phosphoethanolamine, glycerol 3-phosphate and glycerophosphocholine. L-aspartate was down-regulated in LPS12h and LPS24h compared to Control ($p < 0.05$) and showed a decrease in LPS24h compared to LPS12h as well ($p < 0.05$). Some metabolites, including PGG2 and 15-keto-PGE2 in LPS12h increased highly significantly when compared to Control ($p < 0.01$) but showed a highly significant reduction in LPS24h when compared with LPS12h ($p < 0.01$). The metabolites α -linolenic acid (α -LA) and linoleic acid (LA) significantly decreased in LPS12h compared to Control ($p < 0.05$). More information of differential metabolites between groups are summarized in Supplementary Tables S1, S2 and S3.

Characterization and functional analysis of the key metabolic pathways involved in bMECs inflammation. Based on the Impact and *p* values, 42 metabolic pathways in which potential biomarkers might be located were mapped by MetaboAnalyst (Fig. 6). The pathways in which both Impact > 0.1 and $p < 0.05$ were considered as the highest potential metabolic pathways, among which 3 pathways had Impact of 1: D-glutamine and D-glutamic acid metabolism; Linoleic acid metabolism; and α -linolenic acid metabolism (Table 2).

Interrelation maps of the differential metabolites in the main metabolic pathways were generated by analyzing Kyoto Encyclopedia of Genes and Genomes (KEGG) pathway database and publications (Fig. 7). The glycerophospholipid metabolic pathway can be associated with glycolysis and glycerolipid metabolic pathways via phosphoglycerate. Phosphatidylcholine in the glycerophospholipid metabolic pathway can generate α -LA and LA, thereby affecting α -LA and LA metabolic pathways. Glutamine is not only a metabolite in the purine metabolic pathway, but also participates in the metabolism of arginine and valine; as well as alanine, aspartic acid,

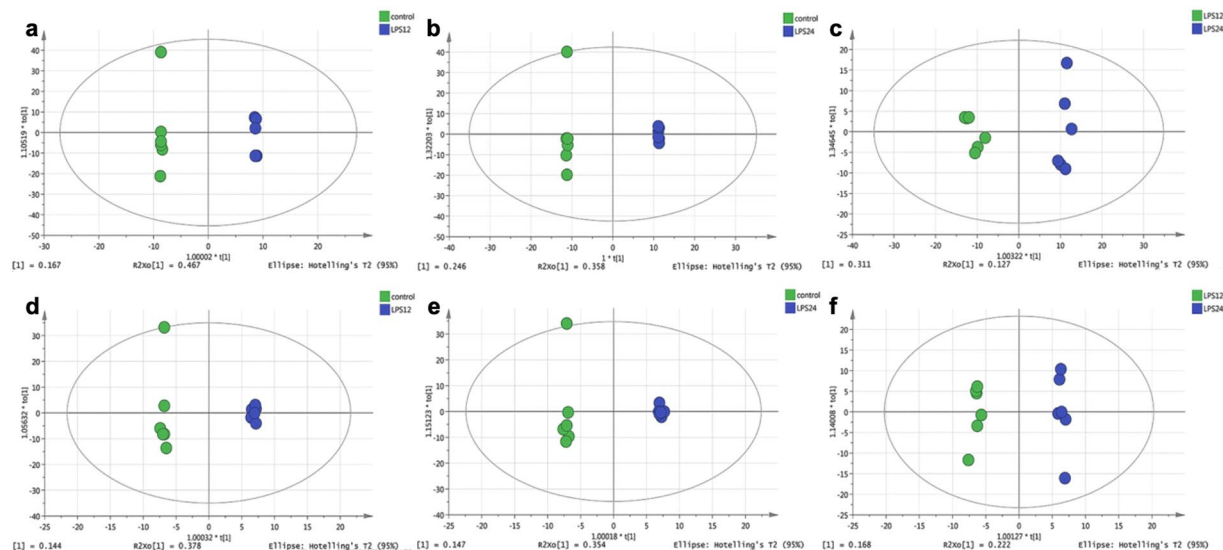


Figure 3. OPLS-DA score plots of all groups. (a–c) Are the OPLS-DA score plots between LPS12h and Control, LPS24h and Control, LPS12h and LPS24h in ESI+, respectively; (d–f) are the OPLS-DA score plots between LPS12h and Control, LPS24h and Control, LPS12h and LPS24h in ESI-, respectively.

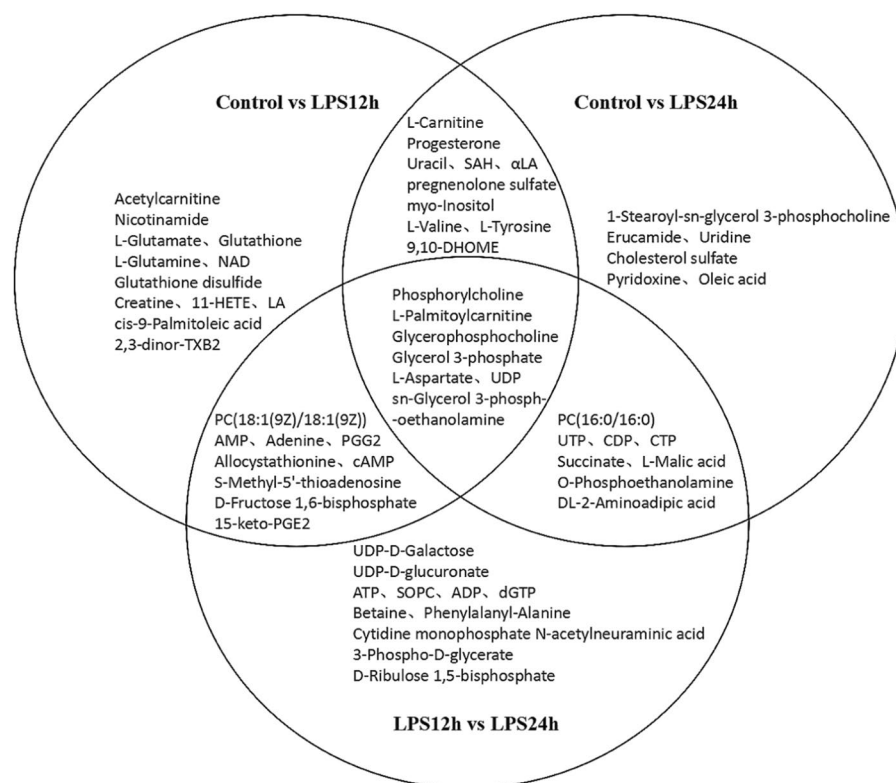


Figure 4. Detection of significant differential metabolites in different groups. NAD: Nicotinamide-adenine dinucleotide; 11HETE: 11-Hydroxyeicosatetraenoic acid; LA: Linoleic acid; 2,3-dinor-TXB2: 2,3-dinor-thromboxane B2; PC: Phosphatidylcholine; PGG2: Prostaglandin G2; cAMP: cyclic Adenosine monophosphate; 15-keto-PGE2: 15-keto Prostaglandin E2; SAH: S-Adenosylhomocysteine; α LA: alpha-Linolenic acid; 9,10-DHOME: 9,10-dihydroxy-12Z-octadecenoic acid; UDP: Uridine diphosphate; UTP: Uridine triphosphate; CDP: Cytidine diphosphate; CTP: Cytidine triphosphate; ATP: Adenosine triphosphate; SOPC: 1-stearoyl-2-oleoyl-sn-glycerol-phosphocholine; ADP: Adenosine diphosphate; dGTP: Deoxyguanosine triphosphate.

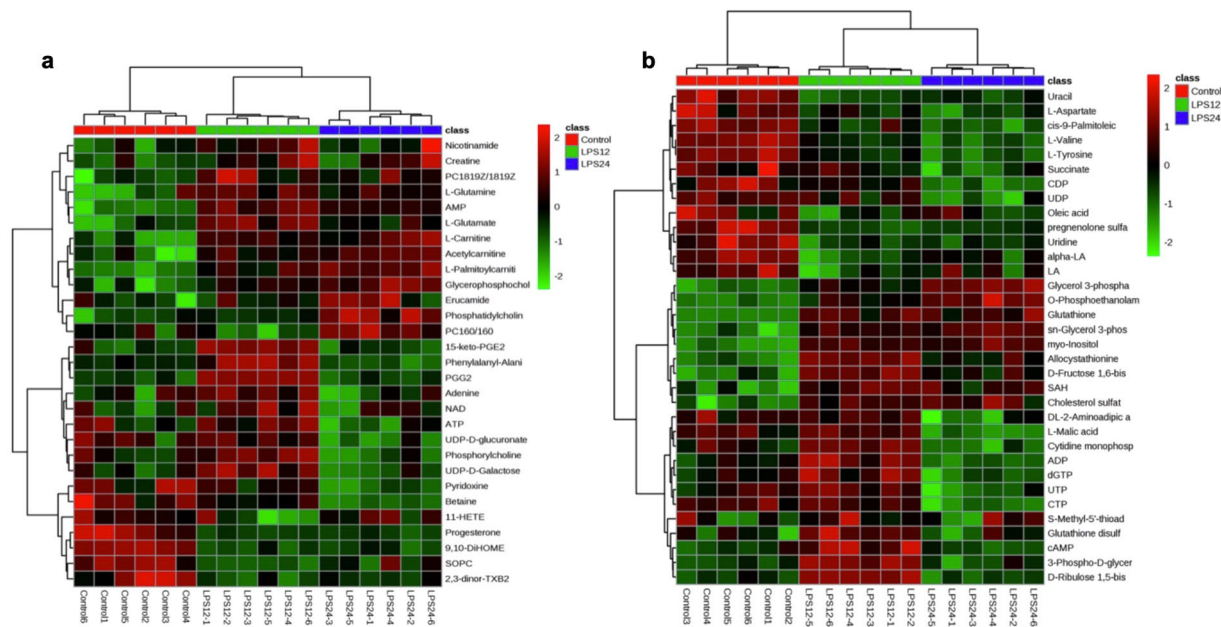


Figure 5. Hierarchical clustering of differential metabolites. **(a)** Hierarchical clustering of 29 differential metabolites in ESI+. **(b)** Hierarchical clustering of 34 differential metabolites in ESI-.

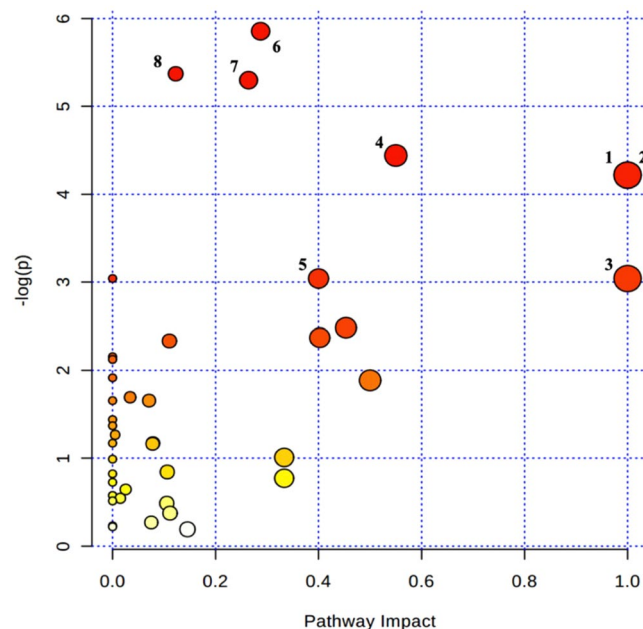


Figure 6. Metabolic pathway analysis. Circles represent metabolic pathways. Darker circles indicate more significant changes in the metabolites in the corresponding pathway, whereas the size of the circle corresponds to the Impact.

and glutamate metabolism. Glutamate is involved in the formation of glutathione, and is not only closely related to glutamine, but also can be metabolized to succinate, participating the metabolism of alanine, aspartate and glutamate.

Discussion

In the present study, there were 38 and 31 differential metabolites in LPS12h and LPS24h compared with Control, respectively, and 35 differential metabolites when LPS12h was compared with LPS24h. Pyrimidine metabolism; purine metabolism; phospholipid metabolism; alanine, aspartate and glutamate metabolism; D-glutamine and D-glutamic acid metabolism; linoleic acid metabolism; ascorbate and aldarate metabolism; and alpha-linolenic

-3-phosphoethanolamine and O-phosphoethanolamine were found to be up-regulated significantly in LPS12h and LPS24h ($p < 0.01$) when compared to Control. The above findings indicated that after bMECs were stimulated by LPS, PCs, LPCs and other metabolites related to glycerophospholipid metabolism, glycerolipid metabolism and glucose metabolism had played anti-inflammatory, pro-inflammatory, antioxidant and energy-providing roles to regulate the cells, suggesting important functions of these pathways in bovine mammary inflammation.

α -LA and LA belong to ω -3 and ω -6 polyunsaturated fatty acids (PUFA) respectively. Pro-inflammatory and bioactive eicosanoids can be derived from LA¹⁴. α -LA has been shown an anti-inflammatory effect¹⁵, studies showed that increasing α -LA in diets can reduce the expression of the pro-inflammatory cytokine TNF- α , and the secretion of IL-1¹⁶. In the present study, there were significant reductions in α -LA and LA in LPS12h ($p < 0.05$). PGG2 and 15-keto-PGE2 were upregulated highly significantly in LPS12h ($p < 0.01$), consistent with previous studies, which showed that eicosanoids such as PGs are sensitive indicators of inflammation¹. PGG2 is a precursor of PGE2, which is one of the most classical lipid mediators derived from AA catalyzed by cyclooxygenases (COXs). It is involved in acute inflammation or inflammatory immune diseases through several mechanisms, enhancing cytokine signaling by regulation of gene expression¹⁷. 15-keto-PGE2 is one of the metabolites of PGE2, which has been reported to down-regulate the expression of pro-inflammatory cytokines, to increase antioxidative transcription factor and nuclear related factor-2 (NRF2), to enhance the reactivity of antioxidation response, and to up-regulate the expression of antioxidant-related genes¹⁸. PGG2 and 15-keto-PGE2 decreased significantly in LPS24h relative to LPS12h ($p < 0.01$), suggesting that the anti-inflammatory or pro-resolving pathways might play a dominant role 24 h after LPS stimulation as the cells are likely restoring homeostasis. In addition to producing pro-inflammatory mediators, LA and α -LA are also precursors of AA, EPA and DHA respectively, which can be derived into anti-inflammatory or pro-resolving mediators¹⁹. It has been shown that patients with moderate or severe asthma and chronic obstructive pneumonia had lower levels of 11-HETE²⁰, consistent with the significantly lower values in LPS12h in our study ($p < 0.05$). These findings show that there were strong immune responses characterized by enhanced α -LA and LA metabolism pathways in bMECs after LPS stimulation.

Among other lipids, there were significant changes in cis-9-palmitoleic acid, L-carnitine, acetylcarnitine and oleic acid. Palmitoleic acid is a monounsaturated fatty acid that can affect inflammatory markers, fat formation and peroxisome proliferator-activated receptor (PPAR) metabolic pathways²¹. It has been reported as having certain therapeutic effects in diseases such as metabolic syndrome, diabetes, inflammation and obesity²², affecting cellular lipid metabolism²³, and improving glucose balance in the body²⁴. Another monounsaturated fatty acid that was found to be differentially produced in the present study is oleic acid. Oleic acid-rich olive oil has proven not only to promote wound healing, but also to be beneficial for cancer, autoimmune and inflammatory diseases. Dietary oleic acid-rich olive oil can eliminate pathogens by interfering with macrophages, lymphocytes and neutrophils²⁵. Cis-9-palmitoleic acid and oleic acid were down-regulated in bMECs after LPS stimulation, indicating enhanced lipid metabolism. This might suggest metabolic consumptions of them in the cells to play anti-inflammatory effect. Carnitine is an important factor in the metabolism of fatty acids in mammals, transferring fatty acids for decomposition, and is often used as a dietary supplement and food antioxidant. L-carnitine was highly significantly increased ($p < 0.01$) in LPS12h and LPS24h in this study. However, Xi *et al.*⁷ reported that carnitine metabolism was down-regulated during mastitis. Acetylcarnitine, which is close related to carnitine, was significantly increased in LPS12h as well ($p < 0.01$). This metabolite has been shown to be effective against pain caused by peripheral neuropathy, the pathogenesis of which includes inflammation²⁶. It has been proposed as a potential biomarkers of allergic asthma and it also plays an important role in the insulin resistance pathway²⁷. These findings might indicate the role of these lipids in anti-inflammatory, antioxidant and energy-regulating functions in the response of bMECs to LPS. They are consistent with the results from an earlier study which indicated that the synthesis of protein and fat in bMECs could be affected by LPS⁶.

Oxygen free-radicals and lipid peroxides can cause oxidative damage to cells. In the present study, the antioxidant pathways such as ascorbate metabolism and glutathione metabolism were affected significantly in bMECs after LPS stimulation. Myo-inositol participates in the process of biosynthesis of ascorbic acid, which functions as an antioxidant and is also very important for immune system. It was significantly up-regulated in LPS12h ($p < 0.05$) and LPS24h ($p < 0.01$) compared to Control, which is consistent with a study of RAW 264.7 showing a significant increase of myo-inositol after LPS stimulation²⁸. UDP-D-glucuronate, also involved in ascorbate metabolism, decreased in LPS24h when compared to LPS12h ($p < 0.05$), as did one of its substrates - UDP-D-galactose. Glutathione, a classical antioxidant with antioxidative stress and detoxification effects which helps maintain the normal function of the immune system²⁹, increased highly significantly in the cells in LPS12h ($p < 0.01$). Glutathione disulfide, a cofactor of glutathione peroxidase³⁰ that has been reported to be involved with glutathione in the biosynthesis of leukotrienes³¹, was highly significantly up-regulated in LPS12h ($p < 0.01$). However, a study on LPS-stimulated macrophages showed that glutathione was the metabolite that decreased most after 6 h LPS stimulation, and the ratio of glutathione and glutathione disulfide also decreased significantly¹³. In the present study, there were significant increases ($p < 0.05$, LPS12h vs Control) in L-glutamate and L-glutamine, which are related to glutathione metabolism. Alanine, aspartate, and glutamate metabolism were all important in LPS-stimulated bMECs, which is consistent with the study of RAW 264.7 cells²⁸, showing this metabolic pathway changed significantly in response to LPS. L-tyrosine was down-regulated in LPS12h and LPS24h, which is in agreement with the observation of the study of Xi *et al.*⁷, showing that milk tyrosine metabolism was altered in mastitis. These findings indicated that the metabolic pathways associated with antioxidants can be rapidly activated in bMECs after LPS stimulation, potentially producing antioxidants to remove excess oxygen free radicals, restoring normal operation of immune system, and maintaining or restoring the redox balance in bMECs during LPS-induced inflammation.

Amino acids are not only essential for protein synthesis in cell metabolism, but also act as intermediate metabolites that promote other biosynthetic reactions. It has been found that amino acid biosynthetic pathways are activated in cancer, and that specific amino acids are produced as important biomolecules such as the

intermediates of nucleotides, lipids and glutathione³². Creatine is an amino acid derivative that is necessary for the rapid synthesis of ATP to supply energy. It is also a metabolite in the biosynthesis of arginine, an amino acid that has antioxidant properties^{5,33}, as well as anti-inflammatory effects³⁴. In the present study, creatine increased significantly in LPS12h ($p < 0.05$), which is consistent with LPS-stimulated RAW 264.7 cells²⁸. L-aspartate and betaine have the ability to act against oxidation and inflammation^{35,36}. Betaine decreased significantly in LPS24h compared to LPS12h ($p < 0.05$). L-aspartate decreased in LPS12h compared to Control ($p < 0.05$) and it reduced significantly in LPS24 compared to LPS12h ($p < 0.01$). Nicotinamide increased significantly in LPS12h ($p < 0.05$). Nicotinamide is the major source of NAD, is a key component of energy metabolism and signaling pathways. It is also an amide derivative of VB3, which has anti-inflammatory effect³⁷. Nicotinamide can also inhibit the secretion of inflammatory cytokines and COXs-derived metabolites³⁸. S-adenosylhomocysteine (SAH), one of key components in methionine cycle, increased significantly in macrophages after 6h LPS stimulation¹³. In the present study, SAH significantly increased in LPS12h and LPS24h when compared to Control ($p < 0.01$). These results suggested that the energy metabolism of bMECs might be enhanced due to LPS stimulation, and metabolites with anti-inflammatory and antioxidant abilities could also be regulated through other pathways to play an important role in bMECs.

Conclusion

In this study, an untargeted metabolomics method was used to analyze the expression pattern of metabolites in bMECs by LPS stimulation. 63 significant differential metabolites were identified. These differential metabolites were primarily involved in eight pathways including lipid metabolism and energy metabolism. The results suggested that bMECs can regulate pro-inflammatory, anti-inflammatory and antioxidant related metabolites to respond to inflammatory stimuli and promote cell homeostasis. Further studies are recommended using targeted metabolomics, lipidomics or proteomics to analyze the potential biomarkers and metabolic pathways identified in this trial, in order to provide screening biomarkers and therapeutic targets for bovine mammary gland inflammation.

Methods

Materials and study design. The cells used in this experiment were the 4th passage of primary bovine mammary epithelial cells stored in the laboratory, which were isolated from healthy multiparous lactating Holstein cows using a procedure described previously³⁹, and were purified and identified before storage. The purity of the cells was assessed at >98%. The cells are in round or elliptical, paving-stone shaped, have rapid proliferation and normal secretion function. The cells were identified by anti-cytokeratin 18 antibody and anti-vimentin antibody purchased from Bioss Biotechnology Co., Ltd (Beijing, China) (Supplementary Figs. S3 and S4). The cells were incubated with DMEM/F12 HEPES supplemented with 10% fetal calf serum after resuscitation. In experiments, they were randomly divided into 3 groups, with 6 biological replicates in each. Then challenged with 500 ng/mL LPS, samples were taken at 0 h, 12 h and 24 h post stimulation, named as Control, LPS12h and LPS24h respectively. In the pilot study, primers were designed with Primer 6.0 and synthesized by Shanghai Sangon Biological Engineering Technology & Services Co. Ltd (Shanghai, China) (Supplementary Table S4). Kits and reagents for all procedures from RNA extraction to RT-qPCR were purchased from TIANGEN Biotech Co., Ltd (Beijing, China) and TakaRa Co. Ltd (Dalian, China). Protein concentration was determined using ELISA assay kits. All the procedures were performed in accordance with the instructions provided by the companies. HPLC-Q-TOF MS detection technology was used in combination with data-dependent acquisition analysis methods to identify differential metabolites from these groups.

Sample preparation and pretreatment. BMECs were washed twice with PBS after removal of the medium, then digested with trypsin and collected in a volume of 1×10^7 cells per sample. After collection, the cells were washed with pre-cooled PBS, and spun at 1,000 r/min for 5 min at 4 °C, washed three times and removed the supernatant. To each sample, 1 mL of methanol: acetonitrile: distilled water (2: 2: 1, v / v) mixture was added to precipitate protein, pulverized by ultrasonic wave at low temperature for 30 min and then allowed them stand at -20 °C for 1 h. After that, samples were centrifuged at 13,000 r/min for 20 min at 4 °C, stored at -80 °C after removing the supernatant and vacuum drying. When dry, 100 μ L of acetonitrile aqueous solution (acetonitrile: water = 1:1, v/v) was added and remixed, following brief vortexing, centrifugation was performed at 14,000 r/min for 15 min at 4 °C, and the supernatant was taken for experiment and analysis.

HPLC-Q-TOF MS analysis. HPLC-Q-TOF MS analysis was performed by Shanghai Applied Protein Technology Co., Ltd. (Shanghai, China) using a 1290 Infinity Ultra-high Performance Liquid Chromatography system (Agilent Technologies, Palo Alto, CA, USA) coupled with a Triple TOF 5600 system (AB/SCIEX, Framingham, MA, USA).

Chromatographic separation was performed on a Waters ACQUITY UPLC BEH Amide 1.7 μ m 2.1 mm \times 100 mm column, and the injection volume was 2 μ L. The column temperature was set at 25 °C and the flow rate was 0.3 mL/min. The mobile phase consisted of A: water + 25 mM ammonium acetate + 25 mM ammonia, and B (acetonitrile). The metabolites were eluted with a gradient of 95% B for 0–1 min; 95% to 65% B for 1–14 min; 65% to 40% B for 14–16 min; maintained at 40% B for 16–18 min; 40% to 95% B for 18–18.1 min; and then maintained at 95% B for 18.1–23 min. During the analysis, samples were placed in 4 °C auto-sampler, and in order to avoid the influence of the instrument detection signal fluctuations, continuous analysis of the samples were performed in a random order. The QC samples were inserted into the samples to monitor system stability and data quality as well.

For MS experiments, this study was conducted using electrospray ionization (ESI) positive and negative ion modes. The ESI source conditions after chromatographic separation were as follows: Ion Source Gas1 (Gas1): 60 psi, Ion Source Gas2 (Gas2): 60 psi, Curtain gas (CUR): 30 psi, source temperature: 600 °C, Ion Spray Voltage

Floating (ISVF) ± 5500 V (\pm ESI); TOF MS scan m/z range: 60–1000 Da, product ion scan m/z range: 25–1000 Da, TOF MS scan accumulation time 0.20 s/spectra, product ion scan accumulation time 0.05 s/spectra; the secondary mass spectra were acquired using information dependent acquisition (IDA) and used the peak intensity screening mode, Declustering potential (DP): ± 60 V (\pm ESI), collision Energy: 35 ± 15 eV, IDA was set to dynamically exclude isotope ions within 4 Da and collect 6 fragment maps per scan.

Data processing and statistical analyses. The data were converted into.mzXML format using ProteoWizard software (Version 3.0, Palo Alto, CA, USA)⁴⁰, peak alignment, retention time correction and peak area extraction were performed using XCMS program⁴¹. Checked the integrity of the data obtained, deleted or supplemented the missing values and deleted the extreme values or ion peaks of which missed values more than 50%. The data of samples and metabolites were normalized to ensure that samples could be compared in parallel.

SIMCA-P (Version 14.1, Umetrics, Umea, Sweden) was used for multivariate statistical analysis. After pareto-scaling, unsupervised PCA was used to analyze the data, including QC samples consisting of 30 μ L per sample, which can be used to detect the status of the instruments, balance the system and evaluate the stability. Tightly clustered QC samples can indicate the repeatability of the test and ensure that the stability of the instrumental analysis system is good, that the data are reliable, so that the differences in the metabolic profiles truly reflect the biological differences among the samples. Subsequently all samples were subjected to PLS-DA and OPLS-DA. Unlike PCA, PLS-DA is a supervised statistical method for discriminant analyses. OPLS-DA is a method that is calibrated on the basis of PLS-DA, filtering out noise that has nothing to do with the information classification, and improving the model's analytical ability and effectiveness. R2Y and Q2 in OPLS-DA represent the rate of model interpretation and model predictive ability respectively, when $1 \geq R2Y$ and $Q2 \geq 0.4$, it indicates that the model is determined to be stable and reliable⁴². The VIP values obtained from OPLS-DA are used to measure the influence and interpretation ability of each metabolite expression pattern on the classification discrimination of each group, thereby assisting in the selection of marker metabolites. Finally, *t*-test and fold change analysis (calculate the average levels of a metabolite in one group relative to the other) were performed.

Potential biomarker screening was performed based on both OPLS-DA VIP > 1 and $p < 0.05$, and were identified by searching an in-house standard MS/MS library and online databases METLIN (<http://metlin.scripps.edu>) and HMDB (<http://www.hmdb.ca>) (using exact mass data (mass error ≤ 25 ppm) or MS/MS spectra matching)⁴¹. The in-house library contains MS/MS spectra of approximately 800 compounds which were obtained from standards. The MS/MS spectra that could not be matched to any of those in the in-house library were searched in online databases. Finally, MetaboAnalyst 4.0 (<http://www.metaboanalyst.ca>) and KEGG (<http://www.genome.jp/kegg>) were processed to cluster analysis and metabolic pathway analysis on differential metabolites.

Data availability

The data used to support the findings of this study are available from the corresponding author by request.

Received: 21 April 2019; Accepted: 30 November 2019;

Published online: 13 December 2019

References

- Piotrowska-Tomala, K. K. *et al.* Lipopolysaccharides, cytokines, and nitric oxide affect secretion of prostaglandins and leukotrienes by bovine mammary gland epithelial cells. *Domest. Anim. Endocrinol.* **43**, 278–288 (2012).
- Deb, R. *et al.* Trends in diagnosis and control of bovine mastitis: a review. *Pak. J. Biol. Sci.* **16**, 1653–61 (2013).
- Gunther, J. *et al.* Comparative kinetics of *Escherichia coli*- and *Staphylococcus aureus*-specific activation of key immune pathways in mammary epithelial cells demonstrates that *S. aureus* elicits a delayed response dominated by interleukin-6 (IL-6) but not by IL-1A or tumor necrosis factor alpha. *Infect. Immun.* **79**, 695–707 (2011).
- Ibega-Awemu, E. M. *et al.* Bacterial lipopolysaccharide induces increased expression of toll-like receptor (TLR) 4 and downstream TLR signaling molecules in bovine mammary epithelial cells. *Vet. Res.* **39**, 11–22 (2008).
- Wu, T. *et al.* Arginine Relieves the Inflammatory Response and Enhances the Casein Expression in Bovine Mammary Epithelial Cells Induced by Lipopolysaccharide. *Mediators Inflamm.*, **2016**; <https://doi.org/10.1155/2016/9618795> (2016).
- Li, L., Tang, J., Wu, J. & Wang, G. Analysis of expression protein profiles of bovine mammary epithelial cell based on isobaric tag for relative and absolute quantification proteomics and bioinformatics technique. *Acta Veterinaria et Zootechnica Sinica.* **47**, 1853–1860 (2016).
- Xi, X. *et al.* Ultra-performance liquid chromatography-quadrupole-time of flight mass spectrometry MS(E)-based untargeted milk metabolomics in dairy cows with subclinical or clinical mastitis. *J. Dairy Sci.* **100**, 4884–4896 (2017).
- Yuan, A. *et al.* Revealing anti-inflammation mechanism of water-extract and oil of *forsythiae fructus* on carrageenan-Induced edema rats by serum metabolomics. *Biomed. Pharmacother.* **95**, 929–937 (2017).
- Chakravarthy, M. V. *et al.* Identification of a physiologically relevant endogenous ligand for PPARalpha in liver. *Cell.* **138**, 476–488 (2009).
- Zhang, Y. *et al.* Protective Effect of Phosphatidylcholine on Restoration of Ethanol-Injured Hepatocytes Related with Caveolin-1. *J. Membr. Biol.* **247**, 73–80 (2014).
- Yan, J. J. *et al.* Therapeutic effects of lysophosphatidylcholine in experimental sepsis. *Nat. Med.* **10**, 161–167 (2004).
- Zalewski, A. & Macphee, C. Role of lipoprotein-associated phospholipase A2 in atherosclerosis: biology, epidemiology, and possible therapeutic target. *Arterioscler. Thromb. Vasc. Biol.* **25**, 923–931 (2005).
- Yu, W. *et al.* One-Carbon Metabolism Supports S-Adenosylmethionine and Histone Methylation to Drive Inflammatory Macrophages. *Mol Cell.* **75**, 1147–1160 e1145; <https://doi.org/10.1016/j.molcel.2019.06.039> (2019).
- Wanten, G. J. A. & Calder, P. C. Immune modulation by parenteral lipid emulsions. *Am. J. Clin. Nutr.* **85**, 1171–1184 (2007).
- Anand, R. & Kaithwas, G. Anti-inflammatory potential of alpha-linolenic acid mediated through selective COX inhibition: computational and experimental data. *Inflammation.* **37**, 1297–1306 (2014).
- Rezamand, P., Hatch, B. P., Carnahan, K. G. & McGuire, M. A. Effects of alpha-linolenic acid-enriched diets on gene expression of key inflammatory mediators in immune and milk cells obtained from Holstein dairy cows. *J. Dairy Res.* **83**, 20–27 (2016).
- Kawahara, K. *et al.* Prostaglandin E-2-induced inflammation: Relevance of prostaglandin E receptors. *Biochim. Biophys. Acta.* **1851**, 414–421 (2015).

18. Chen, Q., Francis, E., Hu, G. & Chen, L. Metabolomic profiling of women with gestational diabetes mellitus and their offspring: Review of metabolomics studies. *J. Diabetes Complications*. **32**, 512–523 (2018).
19. Serhan, C. N. & Petasis, N. A. Resolvins and Protectins in Inflammation Resolution. *Chem. Rev.* **111**, 5922–5943 (2011).
20. Fritscher, L. G. *et al.* Profile of eicosanoids in breath condensate in asthma and COPD. *J. Breath Res.*, **6**; <https://doi.org/10.1088/1752-7155/6/2/026001> (2012).
21. Zong, G. *et al.* Associations of erythrocyte palmitoleic acid with adipokines, inflammatory markers, and the metabolic syndrome in middle-aged and older Chinese. *Am. J. Clin. Nutr.* **96**, 970–976 (2012).
22. Wu, Y., Li, R. & Hildebrand, D. F. Biosynthesis and metabolic engineering of palmitoleate production, an important contributor to human health and sustainable industry. *Prog. Lipid Res.* **51**, 340–34 (2012).
23. Suzuki, S. *et al.* BDNF-Dependent Accumulation of Palmitoleic Acid in CNS Neurons. *Cell. Mol. Neurobiol.* **32**, 1367–1373 (2012).
24. Bolsoni-Lopes, A. *et al.* Palmitoleic acid (n-7) increases white adipocytes GLUT4 content and glucose uptake in association with AMPK activation. *Lipids Health Dis.* **13**, 199–209 (2014).
25. Sales-Campos, H. *et al.* An Overview of the Modulatory Effects of Oleic Acid in Health and Disease. *Mini. Rev. Med. Chem.* **13**, 201–210 (2013).
26. Mostacci, B., Liguori, R. & Cicero, A. F. G. Nutraceutical Approach to Peripheral Neuropathies: Evidence from Clinical Trials. *Curr. Drug Metab.* **19**, 460–468 (2018).
27. Yu, M. *et al.* The Effect of Chinese Herbal Medicine Formula mKG on Allergic Asthma by Regulating Lung and Plasma Metabolic Alterations. *Int. J. Mol. Sci.* **18**, 602–620 (2017).
28. Liu, K. *et al.* Metabolomics Analysis To Evaluate the Anti-Inflammatory Effects of Polyphenols: Glabridin Reversed Metabolism Change Caused by LPS in RAW 264.7 Cells. *J. Agric. Food Chem.* **65**, 6070–6079 (2017).
29. Homma, T. & Fujii, J. Application of Glutathione as Anti-Oxidative and Anti-Aging. *Drugs. Curr. Drug Metab.* **16**, 560–571 (2015).
30. Moloudizargari, M. *et al.* Effects of the polyunsaturated fatty acids, EPA and DHA, on hematological malignancies: a systematic review. *Oncotarget*. **9**, 11858–11875 (2018).
31. Chakouri, N. *et al.* Stress-induced protein S-glutathionylation and phosphorylation crosstalk in cardiac sarcomeric proteins - Impact on heart function. *Int. J. Cardiol.* **258**, 207–216 (2018).
32. Tsun, Z.-Y. & Possemato, R. Amino acid management in cancer. *Semin. Cell Dev. Biol.* **43**, 22–32 (2015).
33. Tripathi, P. & Pandey, S. L-Arginine attenuates oxidative stress condition during cardiomyopathy. *Indian J. Biochem. Biophys.* **50**, 99–104 (2013).
34. Riesberg, L. A. *et al.* Beyond muscles: The untapped potential of creatine. *Int. Immunopharmacol.* **37**, 31–42 (2016).
35. Ahn, M. *et al.* Hepatoprotective effects of Lycium chinense Miller fruit and its constituent betaine in CCl4-induced hepatic damage in rats. *Acta. Histochem.* **116**, 1104–1112 (2014).
36. Leng, W. *et al.* Aspartate alleviates liver injury and regulates mRNA expressions of TLR4 and NOD signaling-related genes in weaned pigs after lipopolysaccharide challenge. *J. Nutr. l Biochem.* **25**, 592–599 (2014).
37. Kao, S.-J., Liu, D. D., Su, C.-F. & Chen, H. I. Niacinamide abrogates the organ dysfunction and acute lung injury caused by endotoxin. *Journal of Cardiovascular Pharmacology* **50**, 333–342 (2007).
38. Weiss, R. *et al.* Nicotinamide: a vitamin able to shift macrophage differentiation toward macrophages with restricted inflammatory features. *Innate Immunity* **21**, 813–826 (2015).
39. Hu, H. *et al.* In vitro culture and characterization of a mammary epithelial cell line from Chinese Holstein dairy cow. *PLoS One* **4**, e7636, <https://doi.org/10.1371/journal.pone.0007636> (2009).
40. Chambers, M. C. *et al.* A cross-platform toolkit for mass spectrometry and proteomics. *Nat. Biotechnol.* **30**, 918–920 (2012).
41. Jia, H. *et al.* Predicting the pathological response to neoadjuvant chemoradiation using untargeted metabolomics in locally advanced rectal cancer. *Radiother. Oncol.* **128**, 548–556 (2018).
42. Westerhuis, J. A. *et al.* Assessment of PLS-DA cross validation. *Metabolomics*. **4**, 81–89 (2008).

Acknowledgements

This project was supported by the Double Subject Construction Plan of Sichuan Agricultural University (No. 03571537). HPLC-Q-TOF MS analysis in this study was supported by Shanghai Applied Protein Technology Co. Ltd (Shanghai, China). Thanks to Professor Nicholas Jonsson from University of Glasgow for his comments on this manuscript and language editing.

Author contributions

Y.X. Huang, L.H. Shen and S.Z. Cao conceived and designed the study. Y.X. Huang, J. Jiang, Q.P. Xu, Q. Luo, S.M. Yu, X.P. Yao, Z.H. Ren and Y.C. Hu performed the study. Y.X. Huang, L.H. Shen, Z.Z. Luo, Y.X. Yang and S.Z. Cao analyzed and prepared the manuscript. All authors reviewed the manuscript.

Competing interests

The authors declare no competing interests.

Additional information

Supplementary information is available for this paper at <https://doi.org/10.1038/s41598-019-55556-2>.

Correspondence and requests for materials should be addressed to S.C.

Reprints and permissions information is available at www.nature.com/reprints.

Our study was performed in strict accordance with the guidelines of the Care and Use of Laboratory Animals of China, and all procedures were approved by the Animal Care and Use Committee of Sichuan Agricultural University.

Publisher's note Springer Nature remains neutral with regard to jurisdictional claims in published maps and institutional affiliations.



Open Access This article is licensed under a Creative Commons Attribution 4.0 International License, which permits use, sharing, adaptation, distribution and reproduction in any medium or format, as long as you give appropriate credit to the original author(s) and the source, provide a link to the Creative Commons license, and indicate if changes were made. The images or other third party material in this article are included in the article's Creative Commons license, unless indicated otherwise in a credit line to the material. If material is not included in the article's Creative Commons license and your intended use is not permitted by statutory regulation or exceeds the permitted use, you will need to obtain permission directly from the copyright holder. To view a copy of this license, visit <http://creativecommons.org/licenses/by/4.0/>.

© The Author(s) 2019